Telomere structure and shortening in telomerase-deficient *Trypanosoma brucei*

Oliver Dreesen, Bibo Li and George A. M. Cross*

Laboratory of Molecular Parasitology, The Rockefeller University, 1230 York Avenue, NY 10021-6399, USA

GenBank accession no: AY904042

ABSTRACT

Telomerase consists of a reverse transcriptase (TERT) and an RNA that contains a template for telomere-repeat extension. Telomerase is required to prevent telomere erosion and its activity or lack thereof is important for tumorigenesis and ageing. Telomerase has been identified in numerous organisms but it has not been studied in kinetoplastid protozoa. *Trypanosoma brucei,* the causative agent of African sleeping sickness, evades the host immune response by frequently changing its variant surface glycoprotein (VSG). The single expressed *VSG* is transcribed from one of ~20 subtelomeric 'Expression Sites', but the role telomeres might play in regulating *VSG* transcription and switching is unknown. We identified and sequenced the *T.brucei* TERT gene. Deleting TERT resulted in progressive telomere shortening of 3–6 bp per generation. In other organisms, the rate of telomere shortening is proportional to the length of the terminal 3′ single-strand overhang. In *T.brucei,* G-overhangs were undetectable (<30 nt) by in-gel hybridization. The rate of telomere shortening therefore, agrees with the predicted shortening due to the end replication problem, and is consistent with our observation that G-overhangs are short. Trypanosomes whose telomere length can be manipulated provide a new tool to investigate the role of telomeres in antigenic variation.

INTRODUCTION

Telomeres consist of tandem G-rich repeats and ensure genome integrity, by protecting chromosome ends from nucleolytic degradation and illegitimate activation of DNA damage checkpoint pathways (1–3). In most organisms, telomeres are maintained by telomerase, a ribonucleoprotein containing a reverse transcriptase and an RNA (4–6). Telomerase RNA contains a region complementary to ~1.5 telomeric repeats that serves as a template for TERT to add hexameric repeats to the telomere terminal 3′ single-stranded overhang (7).

TERT has been identified in many organisms, including *Schizosaccharomyces pombe*, mammals (4,5), *Tetrahymena* (8) and plants (9,10), indicating that telomerase is a highly conserved feature of eukaryotic cells. Telomerase activity is tightly regulated through a variety of telomere-associated factors, including TRF1, TRF2, hRap1 and Pot1 in human cells, and Rap1, Rif1, Rif2 and Cdc13 in *Saccharomyces cerevisiae* (11).

A major drawback in replicating linear chromosomes—the so-called 'end replication problem'—was recognized by Watson (12), who predicted that removal of the lagging strand synthesis primer from the end of the telomeres would result in a single-stranded region that could not be duplexed by conventional DNA polymerases. Consequentially, chromosome ends would progressively shorten over time. This prediction was confirmed by the observation that telomeres of somatic human cells progressively shortened during each replication cycle (13). The observed rate of telomere decline correlated with the length of the terminal G-strand overhang (14–16). The eventual consequences of telomere shortening are manifested by cellular senescence and apoptosis (13,17). In contrast to somatic human cells, germline cells and the majority of tumors, as well as unicellular organisms, have an unlimited proliferation capacity and maintain telomere length by constitutively expressing telomerase (18–21).

In this report we describe the identification, characterization and deletion of TERT in *Trypanosoma brucei*, the pathogenic agent of african sleeping sickness and the most evolutionarily divergent eukaryote that has been extensively studied. This kinetoplastid, protozoan parasite persists in its mammalian host by frequently changing its surface coat, which is made of a homogeneous dense layer of variant surface glycoprotein (VSG) (22). *VSG* genes are dispersed around the genome, but the transcribed *VSG* is located in one of ~20 polycistronic subtelomeric transcription units, known as 'Expression Sites'

---

*To whom correspondence should be addressed. Tel: +1 212 327 7571; Fax: +1 212 3277845; Email: george.cross@rockefeller.edu

(ES) (23–25). Transcription occurs exclusively at one of ~20 ES, whereas the remaining 19 are silent. The monoallelic nature of ES transcription remains as one of the most challenging and unsolved problems in trypanosome biology, and telomeres could play an important part in ES regulation. We show, by comparative sequence analysis, that *tb*TERT contains the hallmark reverse transcriptase motifs and the characteristic telomerase T-motif. Using unique *VSG* genes at subtelomeric loci as probes, we monitored the lengths of individual telomeres after deleting *tbTERT*. The rate of telomere shortening correlated precisely with the amount of DNA predicted to be lost due to the end replication problem: 4–6 bp/generation. Potential implications of telomere dysfunction, in the context of antigenic variation, are discussed.

MATERIALS AND METHODS

Trypanosome cell lines and plasmid constructions

Wild-type *T.brucei* bloodstream-forms, strain Lister 427 antigenic type MITat 1.2 clone 221a (26,27), were cultured in HMI-9 at 37°C. This cell line, when engineered to express T7 RNA polymerase, Tet repressor and neomycinphospho-transferase, was designated as the bloodstream-form 'single marker' line (28), and was cultured in HMI-9 containing 2.5 µg/ml G418 (Sigma).

Homozygous *TERT* deletion mutants were generated by sequentially replacing the two alleles with genes encoding resistance to Puromycin and Hygromycin, by a double crossover event, using the *TERT* 5′- and 3′-untranslated regions (5′- and 3′-UTRs) as targeting sequences. The UTRs were amplified by PCR from genomic DNA. NotI and PmeI sites (boldface) were included to facilitate subsequent cloning steps: 5′-UTR upper primer; **GCGGCCGC**AATGCTGTTT-CTGTCTGCATAA: 5′-UTR lower primer; **GTTTAAAC**G-TAGTCGGCTGTCCAACGTTAG: 3′-UTR upper primer; **GTTTAAAC**AATGCAAGCTTTTCTCCTTCACGCG: 3′-UTR lower primer: **GCGGCCGC**AATATAAGTAAGG-GAAAGACA. PCR products were cloned into pGEM-T easy (Promega), released by a NotI/PmeI digestion and ligated together into NotI digested, alkaline phosphatase treated pBluescript II SK(+) (Stratagene) creating Vector 2–4. The puromycin *N*-acetyltransferase open reading frame (ORF), flanked by ~100 bp of 5′-and 220 bp of 3′-UTRs from the *T.brucei* actin gene, was released from pHD309-puro. The restriction fragment was blunt ended by DNA Pol I (large Klenow fragment) and ligated into PmeI-digested, dephosphorylated Vector 2–4 creating Vector 2–4-Puro. The gene encoding hygromycin phosphotransferase, plus ~100 bp of 5′-and 300 bp of 3′-UTRs from the *T.brucei* actin gene, was released from pHD309-hygro and ligated into PmeI-digested Vector 2–4 creating Vector 2–4-Hygro. Vectors 2–4-Puro and 2–4-Hygro were digested overnight with NotI, prior to transfection into *T.brucei* single marker cell line as previously described (28).

Alignment of TERT sequences

TERT sequences from *T.brucei, Trypanosoma cruzi* (GenBank ID: Tc00.10470535097456) and *Leishmania major* (GenBank ID: LmjF36.3930) were aligned with TERT characteristic motifs from other organisms, using the ClustalX multiple sequence alignment function of MegAlign software (DNAstar Inc.).

Time course and telomere blots

Telomere length changes were analyzed by culturing parental cells in parallel with heterozygous and homozygous telomerase deletion mutants. Every week, genomic DNA was isolated and genomic blotting and hybridization were performed as described previously (29). Size changes in silent ES telomeres were detected by digesting genomic DNA with the restriction enzymes as indicated in the figures. Terminal restriction fragments containing *VSG* genes were detected as described by Horn *et al*. (30).

G-strand overhang assay

G-strand overhang assays were performed according to a published protocol (31) with minor modifications. Gels were hybridized overnight at 30°C in Church Mix [0.5 M NaPO$_4$ (pH 7.2), 1 mM EDTA (pH 8.0), 7% SDS and 1% BSA]. After washing 3 times for 30 min with 4× SSC (1× SSC is 15 mM tri-sodium citrate and 150 mM NaCl) and once for 30 min with 4× SSC + 0.1% SDS at 20°C, the gel was exposed to a phosphorimager screen for at least 72 h. The gels were then denatured, neutralized and hybridized overnight with the same probes. After washing as described above but at 55°C, the gels were exposed to a phosphorimager screen for 3–5 h.

T.brucei cell and HeLa genomic DNA mixing experiment

To determine whether *T.brucei* cell extracts might degrade G-strand overhangs, *T.brucei* cells were centrifuged and washed twice in 1× TDB [5 mM KCl, 80 mM NaCl, 1 mM MgSO$_4$, 20 mM Na$_2$HPO$_4$, 2 mM NaH$_2$PO$_4$ and 20 mM glucose, (pH 7.7)] then mixed with HeLa DNA at different ratios and DNA was re-isolated as described above. G-overhang assay was performed as described above.

Enzymatic modification of *T.brucei* DNA

DNA was incubated with 30 U of T7 (Gene 6) Exonuclease (US Biochemicals) for 20 min at 37°C or with 20 U of *Escherichia coli* Exonuclease I (US Biochemicals) for 12 h at 37°C (32,33). Overhang assay conditions were the same as above.

RESULTS

Identification and characterization of *T.brucei* TERT

We searched the emerging *T.brucei* genome data for sequences that could encode the characteristic motifs of TERT (6). Our original search yielded a short DNA fragment containing motifs 1, 2, A and B of the reverse transcriptase domains. The complete *TERT* sequence was obtained by sequencing BAC and plasmid clones that covered the telomerase coding region. From these additional sequence data, we were able to assemble a 3579 bp ORF. *T.brucei TERT* is a single-copy gene, located on chromosome 11. It encodes a 132 kDa protein that contains all the domains that are known to be required for catalytic activity (Figure 1). TERT orthologues can be identified in the recently completed
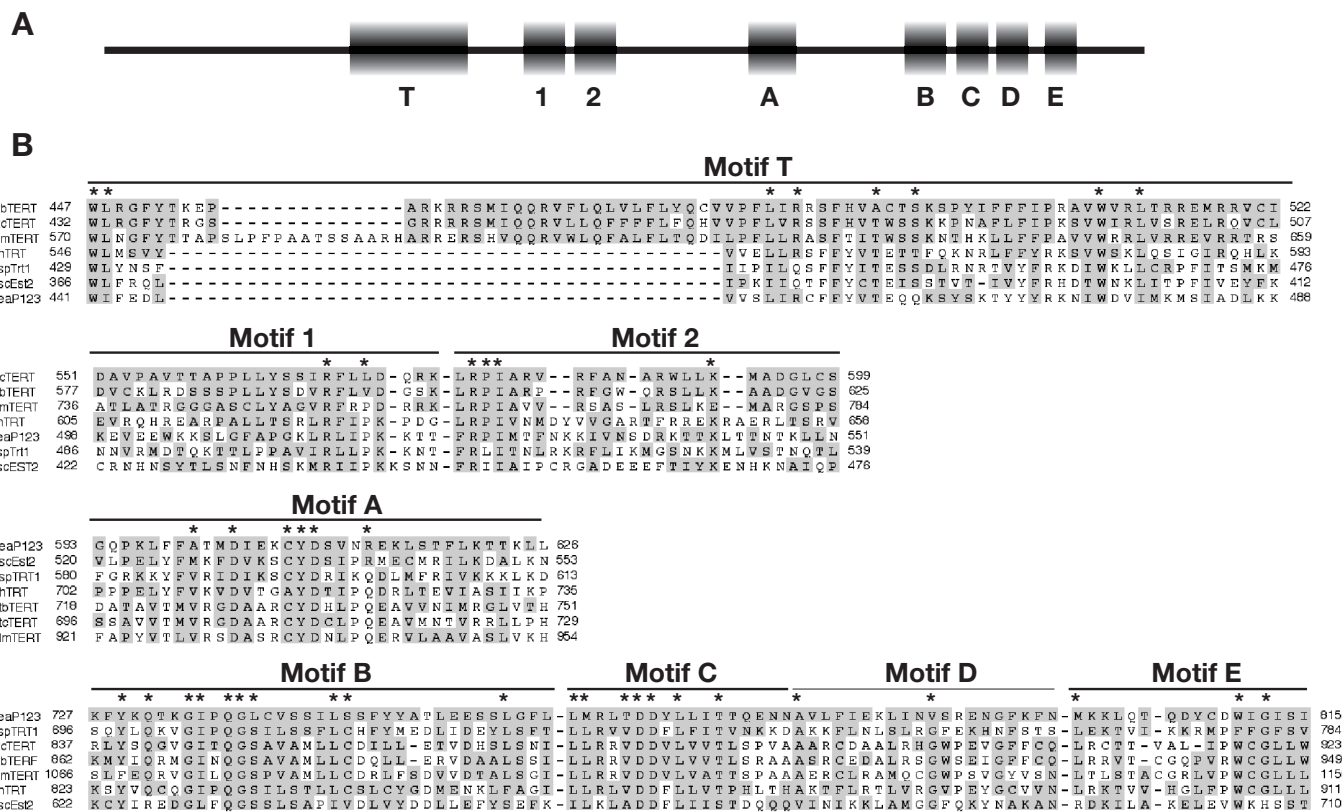
A

```
              T        1   2            A         B  C  D  E
```

B

Motif T

```
tbTERT 447 WLRGFYTKEP-------------ARKRRSMIQQRVFLQLVLFLYQCVVPFLIRRSFHVACTSKSPYIFFFIPRAVWVRLTRREMRRVCI 522
tcTERT 432 WLRGFYTRGS-------------GRRRRSMIQQRVLLQFFFFLFQHVVPFLVRRSFHVTWSSKKPNAFLFIPKSVWIRLVSRELRQVCL 507
lmTERT 570 WLNGFYTTAPSLPFPAATSSAARHARRERSHVQQRVWLQFALFLTQDILPFLLRASFITWSSKNTHKLLFFPAVVWRRLVRREVRRTRS 659
hTRT   546 WLMSVY------------------------------------------------VVELLRSFFYVTETTFQKNRLFFYRKSVWSKLQSIGIRQHLK 593
spTrt1 429 WLYNSF---------------------------------------------------IIPILQSFFYITESSDLRNRTVYFRKDIWKLLCRPFITSMKM 476
scEst2 366 WLFRQL------------------------------------------------IPKIIQTFFYCTEISSTVT-IVYFRHDTWNKLITPFIVEYFK 412
eaP123 441 WIFEDL------------------------------------------------VVSLIRCFFYVTEQQKSYSKTYYYRKNIWDVIMKMSIADLKK 488
```

Motif 1   **Motif 2**

```
tcTERT 551 DAVPAVTTAPPLLYSSIRFLLD-QRK-LRPIARV--RFAN-ARWLLK--MADGLCS 599
tbTERT 577 DVCKLRDSSSPLLYSDVRFLVD-GSK-LRPIARP--RFGW-QRSLLK--AADGVGS 625
lmTERT 736 ATLATRGGGASCLYAGVRFRPD-RRK-LRPIAVV--RSAS-LRSLKE--MARGSPS 784
hTRT   605 EVRQHREARPALLTSRLRFIPK-PDG-LRPIVNMDYVVGARTFRREKRAERLTSRV 658
eaP123 498 KEVEEWKKSLGFAPGKLRLIPK-KTT-FRPIMTFNKKLVNSDRKTTKLTTNTKLLN 551
spTrt1 486 NNVRMDTQKTTLPPAVIRLLPK-KNT-FRLITNLRKRFLIKMGSNKKMLVSTNQTL 539
scEST2 422 CRNHNSYTLSNFNHSKMRIIPKKSNN-FRIIAIPCRGADEEEFTIYKENHKNAIQP 476
```

Motif A

```
eaP123 593 CQPKLFFATMDIEKCYDSVNREKLSTFLKTTKLL 626
scEst2 520 VLPELYFMKFDVKSCYDSIPRMECMRILKDALKN 553
spTRT1 580 FGRKKYFVRIDIKSCYDRIKQDLMFRIVKKKLKD 613
hTRT   702 PPPELYFVKVDVTGAYDTIPQDRLTEVIASIIKP 735
tbTERT 718 DATAVTMVRGDAARCYDHLPQEAVVNIMRGLVTH 751
tcTERT 696 SSAVVTMVRGDAARCYDCLPQEAVMNTVRRLLPH 729
lmTERT 921 FAPYVTLVRSDASRCYDNLPQERVLAAVASLVKH 954
```

Motif B   **Motif C**   **Motif D**   **Motif E**

```
eaP123 727  KFYKQTKGIPQGLCVSSILSSFYYATLEESSLGFL-LMRLTDDYLLITTQENNAVLFIEKLINVSRENGFKPN-MKKLQT-QDYCDWIGISI 815
spTRT1 696  SQYLQKVGIPQGSILSSFLCHFYMEDLIDEYLSFT-LLRVVDDFLFITVNKKDAKKFLNLSLRGFEKHNFSTS-LEKTVI-KKRMPFFGFSV 784
tcTERT 837  RLYSQGVGITQGSAVAMLLCDILL-ETVDHSLSNI-LLRRVDDVLVVTLSPVAAARCDAALRHGWPEVGFFCQ-LRCTT-VAL-IPWCGLLW 923
tbTERF 862  KMYIQRMGINQGSAVAMLLCDQLL-ERVDAALSSI-LLRRVDDVLVVTLSRAAASRCEDALRSGWSEIGPFCQ-LRRVT-CGQPVRWCGLLW 949
lmTERT 1086 SLFEQRVGILQGSPVAMLLCDRLFSDVVDTALSGI-LLRRVDDVLVATTSPAAAERCLRAMQCGWPSVGYVSN-LTLSTACGRLVPWCGLLL 1155
hTRT   823  KSYVQCQGIPQGSILSTLLCSLCYGDMENKLFAGI-LLRLVDDFLLVTPHLTHAKTFLRTLVRGVPEYGCVVN-LRKTVV-HGLFPWCGLLL 911
scEst2 622  KCYIREDGLFQGSSLSAPIVDLVYDDLLEFYSEFK-ILKLADDFLIISTDQQQVINIKKLAMGGFQKYNAKAN-RDKILA-KELEVWKHSST 710
```

Figure 1. Alignment of TERT motifs. (**A**) Schematic representation of the telomerase-specific T-motif and the conserved reverse transcriptase motifs 1, 2, A through E in *T.brucei* TERT. (**B**) Alignment of telomerase-specific motifs of *T.brucei* (*tb*TERT), *T.cruzi* (*tc*TERT), *L.major* (*lm*TERT), *human* (*h*TRT), *S.cerevisiae* (*sc*Est2), *S.pombe* (*sp*Trt1) and *Euplotes aediculatus* TERT (*ea*P123). Sequences of each motif are aligned from top to bottom according to their degree of conservation. Highly conserved residues are marked with an asterisk. Sequence similarities are shaded.

genome sequences of *T.cruzi* (49.1% identity to *tb*TERT) and *L.major* (33.6% identity), the causative agents of Chagas' disease and cutaneous Leishmaniasis, respectively. In contrast, *tb*TERT shows weak sequence identity with human TERT (15.6%), reflecting the early divergence of *T.brucei* in the evolutionary tree (34). Within the T-motif, the three kinetoplastid protozoa contained a highly conserved insertion, of unknown function, that is not present in other organisms. We used RT–PCR to verify that this insertion was present in the mRNA and did not represent an intron in the genomic sequence. To test whether transcription of the *TERT* locus varies between different life cycle stages of the parasite, we isolated mRNA from procyclic (tsetse midgut stage) and bloodstream trypanosomes. No significant difference in telomerase mRNA levels was observed (data not shown).

Telomerase deficiency results in progressive telomere shortening

We deleted both *TERT* alleles by replacement with Hygromycin and Puromycin resistance markers, confirmed by Southern and northern blotting (data not shown). Δ*TERT* clones showed no growth impairment (data not shown), allowing us to monitor changes in telomere length over long periods. Genomic DNA was isolated on a weekly basis and digested with frequently cutting restriction endonucleases, liberating the uncut repetitive telomere tracts for length analysis on agarose gels. We first visualized the size distribution of all

telomeres, by hybridizing the gel with a radiolabeled $(TTAGGG)_4$ probe (Figure 2). Telomere length initially ranged from 3 to 20 kb, and some telomeres were resolved as discrete bands. Each band displayed a moderate progressive shortening. The lengths of specific telomere bands, of differing size ranges and from different gels, were measured. The shortening rate, determined by linear regression analysis on independent chromosome arms, varied from 3 to 6 bp/population doubling (PD). The range of 3–6 bp/PD represents the accuracy that can be assigned to the measurement.

Telomere shortening at silent expression sites

The presence of unique *VSG* genes in several subtelomeric regions allowed us to measure the shortening rate of individual telomeres. DNA samples from a 220 PD time course were digested with enzymes that cut either upstream (EcoRI for *VSG* bR2) or inside (BglI for *VSG* 1.8) a *VSG* ORF, releasing a terminal restriction fragment that was visualized on a Southern blot using a *VSG* 5′ region as the hybridization probe (Figure 3).

These cells contain four copies of *VSG* 1.8 (Figure 3A and data not shown): two copies are located at chromosome-internal sites and two are subtelomeric. In contrast to the chromosome-internal copies, which do not change in size, the subtelomeric restriction fragments (arrowheads in Figure 3A) gradually shorten. During 220 PD, the terminal restriction fragment shortened by ∼1000 bp, corresponding to
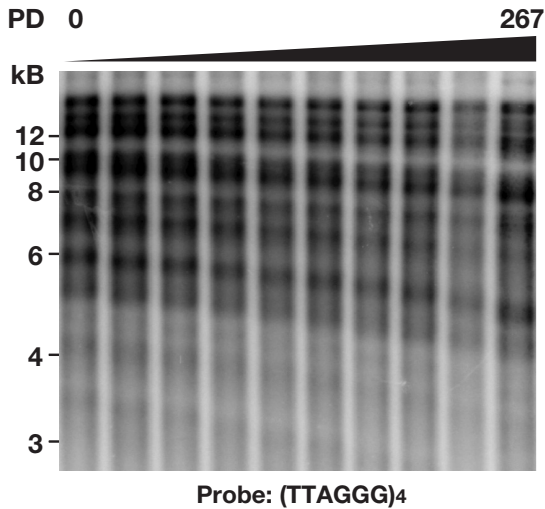
Probe: (TTAGGG)4

Figure 2. Overall telomere shortening in ΔTERT mutants. Over the course of 267 PDs, genomic DNA was isolated at intervals of ~26 PD and digested with MboI and AluI. Terminal restriction fragments were visualized, using a radiolabeled (TTAGGG)4 probe. ImageQuant software (molecular dynamics) was used to distinguish individual bands and determine their shortening rate.
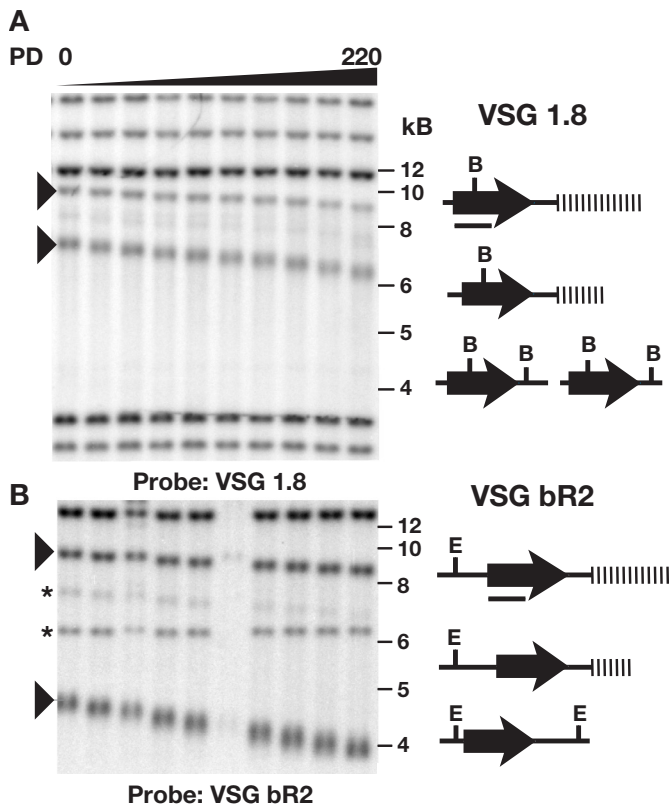

Figure 3. Progressive telomere shortening at silent expression sites. Terminal restriction fragment analysis of silent ES telomeres harboring *VSG* 1.8 (**A**) and *VSG* bR2 (**B**) in the ΔTERT mutant. Time of culturing is indicated in PDs. Telomeric fragments containing *VSG* 1.8 and *VSG* bR2 gradually shorten. Right panel: schematic representation of *VSG* 1.8 and bR2 genes and positions of BglI and EcoRI sites used in the respective DNA digests. Bars indicate the probes used for hybridization. Bands labeled * are due to cross hybridization of the probe with other *VSG*s.

Table 1. Shortening rates at different telomeres in independent experiments

	bp/PD
Bulk telomeres	4.4
	5.6
	5.4
Silent ES telomeres	
VSG bR2	3.5
VSG bR2	4.8
VSG bR2	3.1
VSG 121	3.2
VSG 1.8	4.9
VSG 1.8	4.5

an average telomere shortening rate of ~4.5 bp/PD. Telomere shortening was also observed at *VSG* bR2 ES (Figure 3B). These cells contain three copies of *VSG* bR2 (Figure 3B) two copies are subtelomeric and subject to progressive shortening (marked by arrowheads). Again, telomerase deficiency resulted in a loss of ~950 bp during 220 PD, confirming the shortening rate of 4–5 bp/PD. The results of several independent experiments are summarized in Table 1. To verify that the observed phenotype can be attributed to telomerase deletion, we complemented ΔTERT clones with a tetracycline inducible vector, containing the *tb*TERT ORF. Re-introduction of *tb*TERT, resulted in telomere elongation and reversed the telomere shortening phenotype (data not shown).

We attempted to determine the rate of telomere shortening at the active ES. However, the actively transcribed ES telomere is subject to frequent terminal deletions (35–37), and therefore we could not observe progressive shortening in the absence of telomerase. These frequent truncations and their subsequent repair by telomerase could account for the telomere length heterogeneity, we and others have observed at the active ES in wild-type cells (data not shown) (38).

T.brucei G-strand overhangs are undetectable by conventional in-gel hybridization

In human cells, the rate of telomere shortening in the absence of telomerase correlates with the length of the G-overhang (14,15). In *S.cerevisiae*, telomerase deficiency leads to a telomere decline that correlates precisely with the predicted shortening due to the end replication problem, and with the length of G-overhangs found outside of S-phase (39–41). The moderate telomere shortening rate observed at bulk telomeres and at several silent ES telomeres in telomerase-deficient *T.brucei*, led us to investigate the length of the G-overhangs using a conventional in-gel hybridization assay. This assay permits the detection of single-stranded regions larger than 30 nt on the digested genomic DNA fragments (31).

DNA was digested with frequently cutting restriction enzymes and run in parallel on two agarose gels, which were then dried at room temperature. To detect G-overhangs, one gel was hybridized with a radiolabeled oligonucleotide probe complementary to the G-rich strand [Figure 4, (CCCTAA)4 probe]. As a negative control, and to test whether the DNA denatured during isolation and handling, the duplicate gel was probed with a non-complementary probe [Figure 4, (TTAGGG)4 probe]. To verify equal loading,
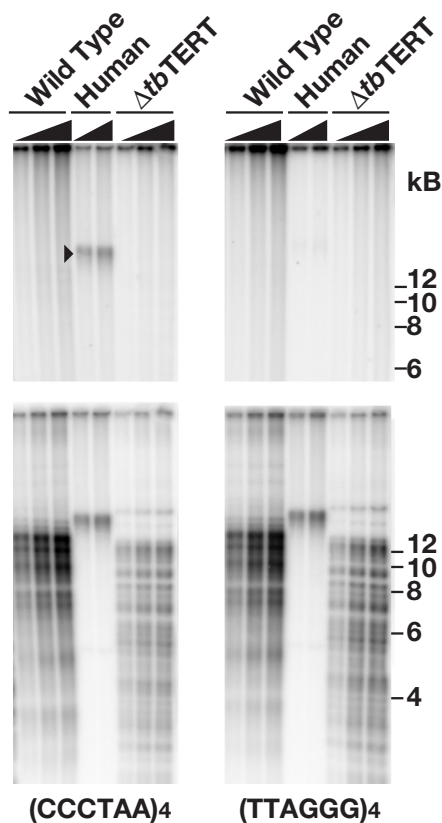
Figure 4. *T.brucei* G-overhangs are undetectable using a conventional in-gel hybridization overhang assay. Overhang assay in wild-type bloodstream *T.brucei*, ΔTERT mutants and human HeLa cells (positive control). Arrows on the top of the gel indicate the increasing amounts of digested DNA loaded onto the gel (wild-type and ΔTERT, 0.5, 1.0 and 1.5 μg; human HeLa DNA, 5.0 and 7.0 μg). Upper panels: native gels were hybridized with (TTAGGG)$_4$ or (CCCTAA)$_4$ probes. The arrowhead indicates the G-overhang detected on human HeLa DNA. Exposure time: 84 h. Lower panels: equal loading of samples was confirmed by denaturation and re-hybridization of the gels. Exposure time: 5 h.

Figure 5. HeLa cell G-overhangs are not degraded during DNA isolation in the presence of *T.brucei* cell extracts. Upper panel lanes 1–6: the proportion of telomeric DNA in *T.brucei* is 100-fold higher than in HeLa cells. The samples contained 0.5, 2.5 or 5.0 μg of MboI- and AluI-digested DNA of HeLa cells (HeLa: lanes 1–3) or wild-type *T.brucei* (BF: lanes 4–6). Upper panel lanes 7–18: the HeLa G-overhang signal is not diminished when telomeres are isolated from mixtures of HeLa DNA and *T.brucei* cells. Increasing numbers of *T.brucei* cells were mixed with 0.5, 2.5 or 5.0 μg HeLa DNA. The amounts of *T.brucei* cells are such that they contributed, to the mixtures, 1.9-, 2.5-, 3- or 3.6-fold as much telomeric DNA as the HeLa cells. Exposure time: 25 h. Lower panel: the same gel after denaturation and re-probing. Increasing amounts of *T.brucei* DNA are evidenced by the characteristic banding pattern of *T.brucei* telomeric DNA. Exposure time: 2 h.

both the gels were denatured and re-probed (Figure 4, lower panels). Due to the large number of minichromosomes, the *T.brucei* samples contain 10- to 100-fold more telomeric DNA than does the same quantity of human DNA. Despite this abundance of chromosome ends, no G-overhang-specific signal was detected by in-gel hybridization. G-overhangs were readily detected on the positive control, human HeLa DNA, as indicated by the arrowhead in Figure 4. Whereas TERT deficiency did not lead to detectable changes in G-overhang length, a slight decline in telomere length and signal intensity were visible (Figure 4, right lanes), as a consequence of telomere shortening during continuous culture. These cells had been in culture for longer than those examined in Figures 2 and 3. We also tested whether G-overhang length varies between *T.brucei* isolated from different life cycle stages. As expected, no significant changes were observed between procyclic and bloodstream trypanosomes (data not shown). These experiments were repeated extensively, using hybridization and washing temperatures that varied from 20 to 50°C and using different *T.brucei* clones, including wild-type isolates, and the results were indistinguishable (data not shown).
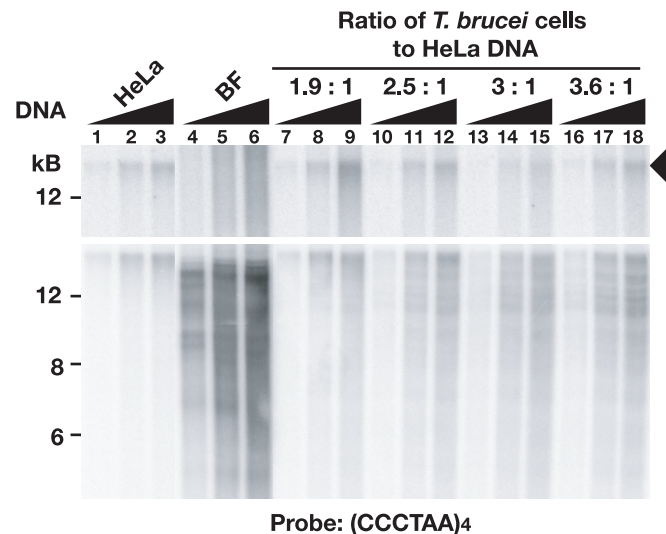
To test whether G-overhangs might have been degraded during DNA isolation, by a hypothetical nuclease activity in the *T.brucei* lysate, we mixed HeLa cell DNA and *T.brucei* cells, then re-isolated DNA from the mixtures, reasoning that the HeLa cell G-overhangs would also be degraded in the mixture (unless the putative nuclease was tightly tethered to trypanosome telomeres, and only acted in *cis*). After DNA isolation, the telomeric tracts were separated on agarose gels and overhang assays were performed (Figure 5, lanes 7–18). The HeLa G-overhang signal (arrowhead) was undiminished after re-isolation in the presence of *T.brucei* cells. Lanes 4–6 confirm that G-overhangs cannot be detected on much larger amounts of *T.brucei* telomeric DNA. The gel was then denatured and re-probed to verify the ratios, as determined by the telomere signal (quantified using a phosphorimager), of *T.brucei* in the mixed samples (Figure 5, lower panel, lanes 7–18). Furthermore, the 100-fold higher relative abundance of telomeric repeats in *T.brucei* DNA is readily apparent when equal amounts of *T.brucei* and HeLa DNA are loaded (Figure 5, lower panel lanes 1–6).

As an additional control, because we could not detect any G-overhang signal on *T.brucei* telomeres (Figure 4), we created artificial G-overhangs by treating *T.brucei* DNA with bacteriophage T7 (Gene 6) 5′ exonuclease (32,33). After enzymatic modification, *T.brucei* DNA was digested to liberate telomeric tracts and a G-overhang-specific signal could be detected by in-gel hybridization using a (CCCTAA)$_4$ probe (Figure 6, upper left panel, two left lanes). The gel distribution of the overhang signal mirrored the distribution of *T.brucei* telomeres, visualized after denaturation and re-probing (lower
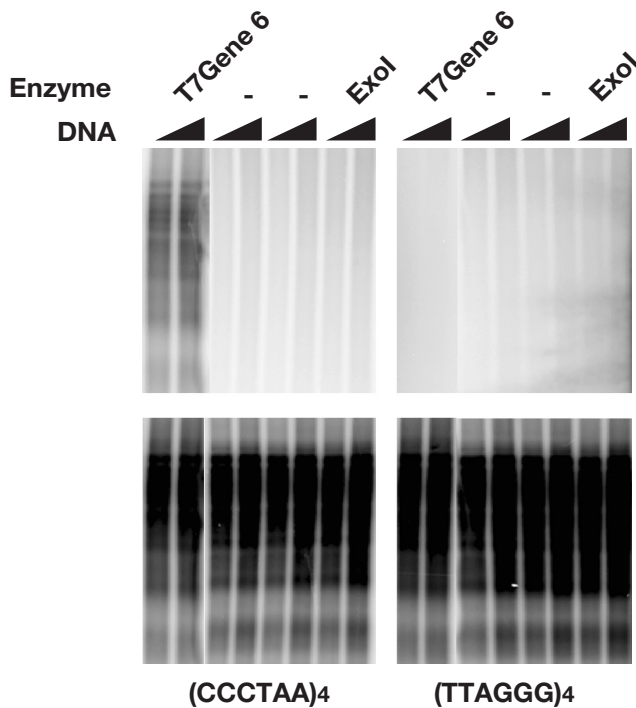
Figure 6. Creation of artificial G-overhangs on *T.brucei* telomeres using bacteriophage T7 5′ exonuclease. Each pair of lanes contains 0.5 or 0.75 μg DNA, untreated (−) or treated with T7 (Gene 6) exonuclease, or exonuclease I. Duplicate gels were hybridized with (CCCTAA)$_4$ (left panel) or (TTAGGG)$_4$ (right panel). Upper panels show hybridization to native gels. A G-strand overhang signal is apparent only after T7 exonuclease digestion (two left lanes). Lower panels show the same gels after denaturation and re-hybridization, to verify the integrity of the telomeric DNA. All panels were exposed for 72 h.

panel), indicating that the G-overhangs were created at telomere termini. To verify that T7 (Gene 6) exonuclease exclusively degraded the C-rich strand and to verify that the DNA remained in its native condition, a duplicate gel was probed with a (TTAGGG)$_4$ probe (Figure 6, upper right panel), which resulted in no hybridization. We also tested whether Exonuclease I, a 3′ single-strand-specific exonuclease, would have any effect on *T.brucei* DNA. As expected, Exonuclease I had no effect on hybridization of probes to either the G or C-rich strands. This experiment shows that artificial G-overhangs can be created on *T.brucei* telomeres *in vitro* and detected by in-gel hybridization, although, the exact size of these overhangs could not be determined.

DISCUSSION

In this study, we characterized *T.brucei TERT* and investigated the effects of its deletion, which resulted in progressive telomere shortening. The rate of erosion was determined for total telomeric tracts, where a few individual telomeres can be visualized as discrete bands. Each band progressively shortened at a rate of 3–6 bp/PD, indicating that telomere shortening is the same at most chromosomes. The subtelomeric location of distinct VSG genes allowed us to confirm this observation at specific telomeres. During several weeks, telomere restriction fragments harboring *VSG*s bR2,

1.8 and 121, also shortened progressively at a steady rate of 3–6 bp/PD.

In contrast to silent ES telomeres, the active ES telomere is affected by frequent truncations [(35,42) and data not shown] and is therefore not informative in regard to progressive telomere erosion. It has been suggested that the instability of the active ES telomere might be a result of its high rate of transcription. Alternatively, these truncations could be the result of active-ES-restricted telomere rapid deletions (43), which can reset the length of over-elongated yeast telomeres to wild-type length and were also proposed to contribute to the size heterogeneity observed at human telomeres (44). However, the nature or the relevance of these truncations at the active *VSG* ES in *T.brucei* remains unclear.

The shortening rate of 3–6 bp/PD is comparable to that observed in telomerase-deficient *S.cerevisiae*, and reflects the amount of telomeric DNA predicted to be lost as a consequence of the end replication problem (39,40). *S.cerevisiae* telomeres acquire readily detectable (>30 nt) G-overhangs in S-phase. During the rest of the cell cycle, G-overhangs are short (41). The overhang length observed outside the S-phase, therefore, correlates with the rate of telomere shortening in the absence of telomerase. A previous study suggested that *T.brucei* telomeres terminate in single-stranded regions that range in size from 75 to 225 nt (29). Therefore, the moderate rate of telomere shortening that we observed in the absence of telomerase led us to investigate G-overhang length, using a conventional in-gel hybridization technique (31). Despite an 10-fold excess in telomeric fragments loaded onto the agarose gel, we were unable to detect any G-overhang signal on wild-type or Δ*TERT* mutants. Furthermore, we showed that any putative *T.brucei* G-overhangs were not being degraded during DNA isolation, and we were easily able to detect artificially created G-overhangs. Taking into consideration the moderate rate of telomere shortening in the absence of telomerase, our results suggest that G-overhangs in proliferating *T.brucei* are short (<30 nt) and therefore, undetectable by conventional in-gel hybridization, and that *T.brucei* might maintain their chromosome ends in a similar fashion to *S.cerevisiae*. While ∼50% of plant chromosome ends harbor overhangs longer than 20–30 nt, the remaining telomeres have overhangs smaller than 12 nt or might be blunt ended (45), and this could also be the case in *T.brucei*. We also cannot exclude the possibility that *T.brucei* telomeres might transiently acquire longer G-overhangs during a particular stage of the cell cycle. However, considering the sensitivity of our assays and the excessive amounts of telomeric fragments loaded onto the gels, we think that this is unlikely.

Mammalian telomeres end in a loop-like structure called the T-loop (33). Subsequent studies on micronuclear chromosomes of *Oxytricha fallax*, *Pisum sativum* and *T.brucei* supported the notion that T-loops are a conserved feature of chromosome ends (29,46,47). T-loops are formed when the single-stranded G-overhang invades upstream repeats by strand displacement. *In vitro* experiments showed that the TTAGGG repeat-binding factor TRF2 enhances loop formation and suggested that a minimal overhang of 6 nt is sufficient for T-loop formation (48). Our data suggest that *T.brucei* G-overhangs are short, yet *T.brucei* telomeres assemble into a T-loop structure. This supports the notion that T-loops can be formed with short overhangs *in vivo*.

Transcription appears to be initiated at every ES promoter, whereas transcriptional elongation occurs exclusively at the active ES (49). It is unclear whether telomere position effect is responsible for transcriptional attenuation at silent ES promoters. Transcription from promoter-reporter cassettes introduced into silent ES, however, is progressively repressed as the insertion site is moved towards the telomere (30). Detailed studies on how telomere length might affect telomere position effect or antigenic variation have been impossible, so far, in part because short telomeres created artificially, which is only possible at the active ES, are rapidly elongated by telomerase (38). However, continued cultivation of ΔTERT cells will eventually produce cells with naturally shortened telomeres at silent ES that can be assessed for possible de-repression of telomere-induced silencing, and for any effect on ES regulation and *VSG* gene conversion. A recent study in telomerase-deficient *Klyuveromyces lactis* showed that short telomeres become highly recombinogenic (50). As telomeres shortens, an initially single-copy subtelomeric marker gene was spread to other chromosome arms by gene conversion. Extrapolating these results into the context of trypanosome antigenic variation, telomere shortening could potentially lead to an enhanced rate of antigenic switching.

The slow loss of telomeric DNA in telomerase-deficient *T.brucei* has been a barrier to study the effect of telomere dysfunction on antigenic variation. However, since the ΔTERT mutant does not show any growth retardation, even after many months of culturing, future experiments are expected to provide valuable insights into the role of telomeres in antigenic variation. Although others have proposed telomerase as a potential drug target for *T.brucei*, our results do not encourage this possibility.

ACKNOWLEDGEMENTS

REFERENCES

1. van Steensel,B., Smogorzewska,A. and de Lange,T. (1998) TRF2 protects human telomeres from end-to-end fusions. *Cell*, **92**, 401–413.
2. de Lange,T. (2002) Protection of mammalian telomeres. *Oncogene*, **21**, 532–540.
3. de Lange,T. (2004) T-loops and the origin of telomeres. *Nature Rev. Mol. Cell Biol.*, **5**, 323–329.
4. Nakamura,T.M., Morin,G.B., Chapman,K.B., Weinrich,S.L., Andrews,W.H., Lingner,J., Harley,C.B. and Cech,T.R. (1997) Telomerase catalytic subunit homologs from fission yeast and human. *Science*, **277**, 955–959.
5. Meyerson,M., Counter,C.M., Eaton,E.N., Ellison,L.W., Steiner,P., Caddle,S.D., Ziaugra,L., Beijersbergen,R.L., Davidoff,M.J., Liu,Q. *et al.* (1997) hEST2, the putative human telomerase catalytic subunit gene, is up-regulated in tumor cells and during immortalization. *Cell*, **90**, 785–795.
6. Lingner,J., Hughes,T.R., Shevchenko,A., Mann,M., Lundblad,V. and Cech,T.R. (1997) Reverse transcriptase motifs in the catalytic subunit of telomerase. *Science*, **276**, 561–567.
7. Greider,C.W. and Blackburn,E.H. (1987) The telomere terminal transferase of *Tetrahymena* is a ribonucleoprotein enzyme with two kinds of primer specificity. *Cell*, **51**, 887–898.
8. Collins,K. and Gandhi,L. (1998) The reverse transcriptase component of the *Tetrahymena* telomerase ribonucleoprotein complex. *Proc. Natl Acad. Sci. USA*, **95**, 8485–8490.
9. Fitzgerald,M.S., Riha,K., Gao,F., Ren,S., McKnight,T.D. and Shippen,D.E. (1999) Disruption of the telomerase catalytic subunit gene from *Arabidopsis* inactivates telomerase and leads to a slow loss of telomeric DNA. *Proc. Natl Acad. Sci. USA*, **96**, 14813–14818.
10. Oguchi,K., Liu,H., Tamura,K. and Takahashi,H. (1999) Molecular cloning and characterization of AtTERT, a telomerase reverse transcriptase homolog in *Arabidopsis thaliana*. *FEBS Lett.*, **457**, 465–469.
11. Smogorzewska,A. and de Lange,T. (2004) Regulation of telomerase by telomeric proteins. *Annu. Rev. Biochem.*, **73**, 177–208.
12. Watson,J.D. (1972) Origin of concatemeric T7 DNA. *Nature New Biol.*, **239**, 197–201.
13. Harley,C.B., Futcher,A.B. and Greider,C.W. (1990) Telomeres shorten during ageing of human fibroblasts. *Nature*, **345**, 458–460.
14. Makarov,V.L., Hirose,Y. and Langmore,J.P. (1997) Long G tails at both ends of human chromosomes suggest a C strand degradation mechanism for telomere shortening. *Cell*, **88**, 657–666.
15. Huffman,K.E., Levene,S.D., Tesmer,V.M., Shay,J.W. and Wright,W.E. (2000) Telomere shortening is proportional to the size of the G-rich telomeric 3′-overhang. *J. Biol. Chem.*, **275**, 19719–19722.
16. Karlseder,J., Smogorzewska,A. and de Lange,T. (2002) Senescence induced by altered telomere state, not telomere loss. *Science*, **295**, 2446–2449.
17. Wong,K.K., Maser,R.S., Bachoo,R.M., Menon,J., Carrasco,D.R., Gu,Y., Alt,F.W. and DePinho,R.A. (2003) Telomere dysfunction and Atm deficiency compromises organ homeostasis and accelerates ageing. *Nature*, **421**, 643–648.
18. de Lange,T. (1994) Activation of telomerase in a human tumor. *Proc. Natl Acad. Sci. USA*, **91**, 2882–2885.
19. Counter,C.M., Hirte,H.W., Bacchetti,S. and Harley,C.B. (1994) Telomerase activity in human ovarian carcinoma. *Proc. Natl Acad. Sci. USA*, **91**, 2900–2904.
20. Kim,N.W., Piatyszek,M.A., Prowse,K.R., Harley,C.B., West,M.D., Ho,P.L., Coviello,G.M., Wright,W.E., Weinrich,S.L. and Shay,J.W. (1994) Specific association of human telomerase activity with immortal cells and cancer. *Science*, **266**, 2011–2015.
21. Sharpless,N.E. and DePinho,R.A. (2004) Telomeres, stem cells, senescence, and cancer. *J. Clin. Invest.*, **113**, 160–168.
22. Hide,G. (1999) History of sleeping sickness in East Africa. *Clin. Microbiol. Rev.*, **12**, 112–125.
23. De Lange,T. and Borst,P. (1982) Genomic environment of the expression-linked extra copies of genes for surface antigens of *Trypanosoma brucei* resembles the end of a chromosome. *Nature*, **299**, 451–453.
24. Bernards,A., Van der Ploeg,L.H., Frasch,A.C., Borst,P., Boothroyd,J.C., Coleman,S. and Cross,G.A.M. (1981) Activation of trypanosome surface glycoprotein genes involves a duplication-transposition leading to an altered 3′ end. *Cell*, **27**, 497–505.
25. Navarro,M. and Cross,G.A. (1996) DNA rearrangements associated with multiple consecutive directed antigenic switches in *Trypanosoma brucei*. *Mol. Cell. Biol.*, **16**, 3615–3625.
26. Doyle,J.J., Hirumi,H., Hirumi,K., Lupton,E.N. and Cross,G.A.M. (1980) Antigenic variation in clones of animal-infective *Trypanosoma brucei* derived and maintained *in vitro*. *Parasitology*, **80**, 359–369.
27. Hirumi,H. and Hirumi,K. (1989) Continuous cultivation of *Trypanosoma brucei* blood stream forms in a medium containing a low concentration of serum protein without feeder cell layers. *J. Parasitol.*, **75**, 985–989.
28. Wirtz,E., Leal,S., Ochatt,C. and Cross,G.A.M. (1999) A tightly regulated inducible expression system for conditional gene knock-outs and dominant-negative genetics in *Trypanosoma brucei*. *Mol. Biochem. Parasitol.*, **99**, 89–101.

29. Munoz-Jordan,J.L., Cross,G.A., de Lange,T. and Griffith,J.D. (2001) t-loops at trypanosome telomeres. *EMBO J*., **20**, 579–588.

30. Horn,D. and Cross,G.A. (1997) Position-dependent and promoter-specific regulation of gene expression in *Trypanosoma brucei*. *EMBO J*., **16**, 7422–7431.

31. Wellinger,R.J., Wolf,A.J. and Zakian,V.A. (1993) *Saccharomyces* telomeres acquire single-strand TG1-3 tails late in S phase. *Cell*, **72**, 51–60.

32. Cimino-Reale,G., Pascale,E., Alvino,E., Starace,G. and D'Ambrosio,E. (2003) Long telomeric C-rich 5′-tails in human replicating cells. *J. Biol. Chem*., **278**, 2136–2140.

33. Griffith,J.D., Comeau,L., Rosenfield,S., Stansel,R.M., Bianchi,A., Moss,H. and de Lange,T. (1999) Mammalian telomeres end in a large duplex loop. *Cell*, **97**, 503–514.

34. Stevens,J.R. and Gibson,W. (1999) The molecular evolution of trypanosomes. *Parasitol. Today*, **15**, 432–437.

35. Bernards,A., Michels,P.A., Lincke,C.R. and Borst,P. (1983) Growth of chromosome ends in multiplying trypanosomes. *Nature*, **303**, 592–597.

36. Pays,E., Laurent,M., Delinte,K., Van Meirvenne,N. and Steinert,M. (1983) Differential size variations between transcriptionally active and inactive telomeres of *Trypanosoma brucei*. *Nucleic Acids Res*., **11**, 8137–8147.

37. Van der Ploeg,L.H., Liu,A.Y. and Borst,P. (1984) Structure of the growing telomeres of Trypanosomes. *Cell*, **36**, 459–468.

38. Horn,D., Spence,C. and Ingram,A.K. (2000) Telomere maintenance and length regulation in *Trypanosoma brucei*. *EMBO J*., **19**, 2332–2339.

39. Lundblad,V. and Szostak,J.W. (1989) A mutant with a defect in telomere elongation leads to senescence in yeast. *Cell*, **57**, 633–643.

40. Singer,M.S. and Gottschling,D.E. (1994) TLC1: template RNA component of *Saccharomyces cerevisiae* telomerase. *Science*, **266**, 404–409.

41. Larrivee,M., LeBel,C. and Wellinger,R.J. (2004) The generation of proper constitutive G-tails on yeast telomeres is dependent on the MRX complex. *Genes Dev*., **18**, 1391–1396.

42. Horn,D. and Cross,G.A.M. (1997) Analysis of *Trypanosoma brucei* vsg expression site switching *in vitro*. *Mol. Biochem. Parasitol*., **84**, 189–201.

43. Li,B. and Lustig,A.J. (1996) A novel mechanism for telomere size control in *Saccharomyces cerevisiae*. *Genes Dev*., **10**, 1310–1326.

44. Li,B. and de Lange,T. (2003) Rap1 affects the length and heterogeneity of human telomeres. *Mol. Biol. Cell*, **14**, 5060–5068.

45. Riha,K., McKnight,T.D., Fajkus,J., Vyskot,B. and Shippen,D.E. (2000) Analysis of the G-overhang structures on plant telomeres: evidence for two distinct telomere architectures. *Plant J*., **23**, 633–641.

46. Cesare,A.J., Quinney,N., Willcox,S., Subramanian,D. and Griffith,J.D. (2003) Telomere looping in *P.sativum* (common garden pea). *Plant J*., **36**, 271–279.

47. Murti,K.G. and Prescott,D.M. (1999) Telomeres of polytene chromosomes in a ciliated protozoan terminate in duplex DNA loops. *Proc. Natl Acad. Sci. USA*, **96**, 14436–14439.

48. Stansel,R.M., de Lange,T. and Griffith,J.D. (2001) T-loop assembly *in vitro* involves binding of TRF2 near the 3′ telomeric overhang. *EMBO J*., **20**, 5532–5540.

49. Vanhamme,L., Poelvoorde,P., Pays,A., Tebabi,P., Van Xong,H. and Pays,E. (2000) Differential RNA elongation controls the variant surface glycoprotein gene expression sites of *Trypanosoma brucei*. *Mol. Microbiol*., **36**, 328–340.

50. McEachern,M.J. and Iyer,S. (2001) Short telomeres in yeast are highly recombinogenic. *Mol. Cell*, **7**, 695–704.